Modeling of Frequency Dependent Losses in Two-port and Three-port Inductors on Silicon

Telesphor Kamgaing, Thomas Myers, Mike Petras, Mel Miller

Motorola SPS, 2100 E. Elliot Road, Mail Drop EL740, Tempe, AZ 85284

Abstract **_New compact model forms for two-port and three-port symmetric inductors fabricated on silicon are discussed in this paper. These new models incorporate a frequency independent RL network that mimics the skin effect behavior of transmission lines on conductive substrates and can accurately predict the inductive behavior as well as the one-port single-ended and the one-port differential Q of these devices at microwave and millimeter wave frequencies. The new models are validated on inductors fabricated in a thick plated copper process.**

I. Introduction

The increasing demand in wireless communication systems has led to more interest in the development of high performance silicon integrated passive components. One of these passive components, which is widely used in front-end transceivers, is the on-chip inductor. Different physical modeling approaches have been demonstrated for on-chip inductors. Early inductor models, such as the conventional PI-model, utilize only frequency independent elements. They model the S-parameters and the inductive behavior of on-chip inductors very well, but fail to provide good modeling of the quality factor Q beyond the peak frequency for low resistivity substrates. Most recently, this conventional PI-model (in one-port configuration) was extended by [1] to include a frequency dependent series resistance that explicitly describes the skin effect. This model offered a significant improvement in modeling the quality factor Q. The explicit frequency dependence of the series resistance, however, prevents the integration of the model in harmonic balanced and time domain simulator such as PSPICE.

To overcome these restrictions, we propose an inductor model that utilizes only frequency independent elements to mimic the skin effect behavior of transmission lines on conductive substrates. The development of the compact model is discussed in section II. Section III presents the experimental results and the model validation.

II. Compact Model Development

The accurate modeling of inductors requires the identification of all model components and their contribution to the device characteristics. In general a good extraction of the series inductance and substrate impedance is sufficient to model the S-parameters, which are less sensitive to the series resistance. Modeling the inductor quality factor, however, demands a more rigorous approximation of the series resistance.

A. Skin Effect Model

A first order approximation of the skin effect of a straight conductor suggests that the resistance of the conductor increases proportionally to the square root of the frequency, whereas the inductance remains almost unchanged. Such a nonlinear behavior is difficult to model with passive components. In addition, for microstip lines on silicon, other effects such as substrate coupling and current crowding at the edges of the conductor make the skin effect even more difficult to understand.

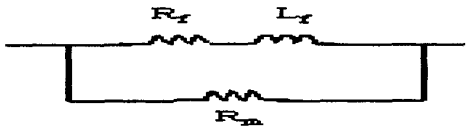

Fig. 1. Compact model of the skin effect

The skin effect modeling of the inductor series resistance is based on the RL network of Fig. 1, where R_m, R_f and L_f are all frequency independent elements. This network was used previously by Kim and Neikirk [2] to model the skin effect of straight conductors in free space and in a dielectric medium.

0-7803-7239-5/02/$10.00 © 2002 IEEE

Its detailed analysis, however, was not performed. Instead, numerical fitting techniques were used to show that adding more series RL elements in parallel to the network provide better accuracy. In this work, we show that with a careful selection of the component values, the single section network of Fig. 1 is sufficient to represent a skin-effect-like behavior of the transmission lines over a large frequency range. The overall impedance of the network of Fig. 1 is given by:

$$Z(j\omega) = R(\omega) + jX(\omega) \qquad (1)$$

where

$$R(\omega) = R_m \cdot \frac{R_m R_f + R_f^2 + \omega^2 L_f^2}{(R_m + R_f)^2 + \omega^2 L_f^2} \qquad (2)$$

and

$$X(\omega) = R_m^2 \cdot \frac{\omega L_f}{(R_m + R_f)^2 + \omega^2 L_f^2} \qquad (3)$$

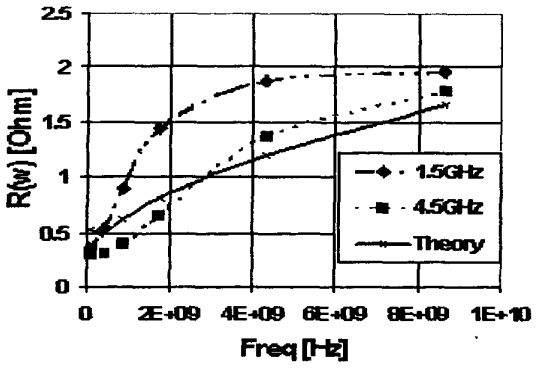

Fig. 2. Calculated R(ω) for network of Fig. 1. R_m=4Ohm and R_f=0.48Ohm and different f_0

Although R(ω) (2) is not proportional to the square-root of the frequency, it begins as $R_m//R_f$ at DC, then increases with the frequency and saturates against R_m at high frequencies. It also has an inflection point, which occurs at the frequency f_0, with

$$\omega_0 = 2\pi \cdot f_0 = \frac{(R_m + R_f)}{\sqrt{3} \cdot L_f} \qquad (4)$$

For given values of R_f and R_m, the value of ω_0, which gives the best approximation of the skin effect is empirically determined. To illustrate this, R(ω) is plotted in Fig. 2 for given values of R_f and R_m against its normalized theoretical value, based on the skin depth formula in [3]. In this example, it can be seen that a f_0 of 4.5GHz provides a better fit. In general, the selection of f_0 is dependent on the device geometry and the frequency range of interest.

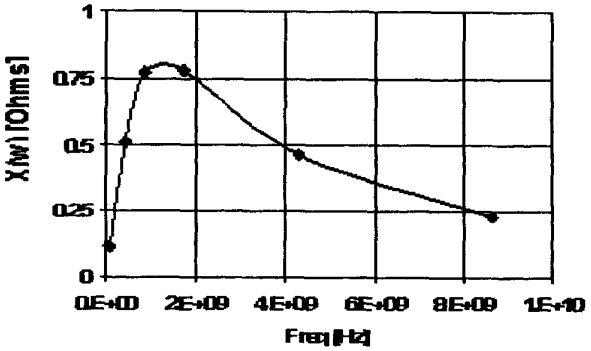

Fig. 3. Calculated X(ω) for network of Fig. 1. with f_0=1.5GHz, R_m=4Ohm and R_f=0.48Ohm

Figure 3 shows X(ω) vs. frequency. It begins very low at DC and peaks at

$$\omega_{peak} = \frac{R_m + R_f}{L_f} = \sqrt{3} \cdot \omega_0 \qquad (5)$$

before dropping again. The value X at ω_{peak} is given by

$$X_{peak} = X(\omega_{peak}) = \frac{1}{2} \cdot \frac{R_m^2}{R_m + R_f} \qquad (6)$$

From equation (3) the resulting frequency dependent inductance

$$L(\omega) = \frac{X(\omega)}{\omega} = \frac{R_m^2 \cdot L_f}{(R_m + R_f)^2 + \omega^2 L_f^2} \qquad (7)$$

decreases quadratically with the frequency and thus has only minor contribution to the overall high-frequency impedance. Indeed, the decrease in inductance with frequency of this network is even stronger than the skin-effect decrease of straight wire inductance as predicted by [4].

A. Two-port Inductor Model

The two-port inductors considered in this study are conventional square and octagonal planar spiral inductors. The new compact model, with two RL networks added to capture the skin effect, is shown in Fig. 4. The original 2-section ladder network (dark) has been discussed previously and can capture

most of the device effects up to the first resonance frequency. In the new model R_f is a fixed percentage of the DC series resistance. The remaining DC resistance is captured by R1.

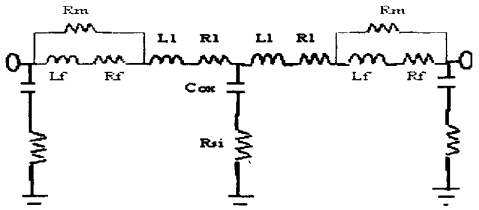

Fig. 4. Skin effect model of two-port inductor

B. Three-port Inductor design and modeling

Three-port symmetric inductors can be used either in place of two symmetric inductors or as a three-terminal (two-port) transformer. The top view of an octagonal three-port inductor is shown in Fig. 5. The device is laid out as a true three-port structure. Here, port 1 and port 2 represent the two ends of the inductors and port 3 is the center tap. This port assignment is adopted throughout the rest of this document.

The equivalent compact model for three-port inductors is shown in figure 6. In addition to the elements of a two-port compact model, it includes the interwinding capacitance Co, which can no longer be neglected with the increasing size of the device and the number of underpasses as well as the close proximity of the two half-inductors. A mutual coupling coefficient term k between L1 and L2 and

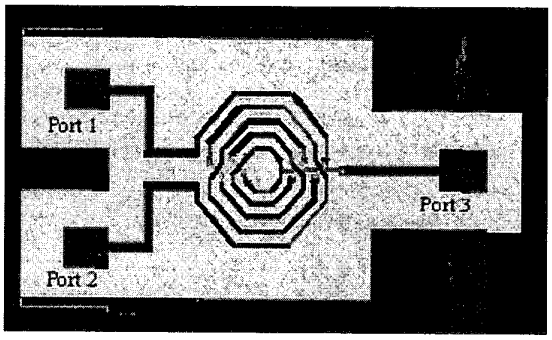

Fig. 5. Top view of an octagonal three-port inductor

an RL series piece (R3-L3) that models the center tap are also added. Since the center tap is relatively short (10 to 100 um) and is usually used as a DC biasing point or RF ground, no skin effect model piece and shunt impedance are needed at port 3.

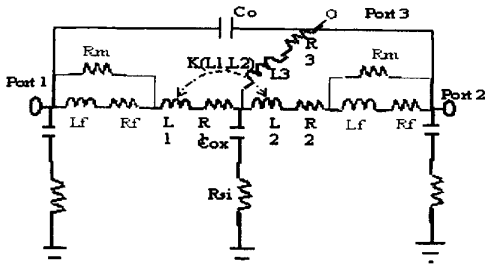

Fig. 6. Skin effect model of three-port inductor

III. Experimental Results

A. Fabrication and Measurements

Square and octagonal spirals with different geometrical attributes were fabricated in Motorola's thick plated copper process.

The RF electrical performance of the two-port inductors was measured using an HP8510C vector network analyzer and ground-signal-ground (GSG) probes. The calibration was carried out with a commercial SOLT calibration substrate from 45MHz to 15GHz in a 50-Ohm environment. The raw S-parameters were subsequently deembedded using ABCD correction techniques.

The three-port inductors were RF characterized using an ATN Microwave multiport system and high-frequency ground-signal-ground-signal-ground (GSGSG) probes. The calibration was also performed with an SOLT calibration substrate from 50MHz to 15GHz in a 50-Ohm environment. The measured data were then reduced by means of Y-parameter correction.

B. Compact Model Validation

Initial values are assigned to the elements of the compact models based on existing inductor libraries. The value of R_f is fixed to 75% of the calculated DC resistance. Numerical fitting, using an in house developed or a commercially available tool, is performed to refine the model element values. The models are extracted up to 8GHz or the lowest resonance frequency of the S-parameters.

The measured vs. modeled S-parameters of a typical 3-port 6nH inductor are shown in Fig. 7. Very good match can be observed between measured and modeled data.

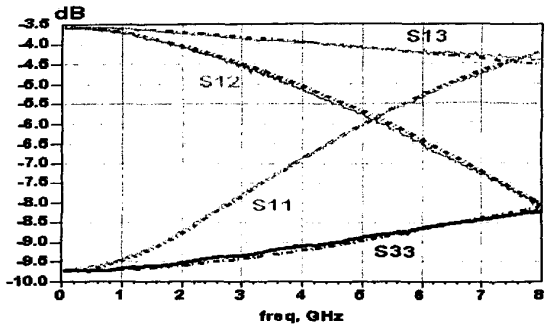

Fig. 7. Measured (solid line) vs. modeled (doted line) S-parameters of a three-port inductor.

Fig. 8 shows the measured vs. modeled one-port and differential Q for different three-port inductors, which were calculated with port 3 open. In differential mode, the peak Q and the device bandwidth are 30 to 40% higher than those of the single-ended mode. A comparison of the new inductor model with the conventional model is shown in figure 9. The most significant improvement is observed in the modeling of the differential Q.

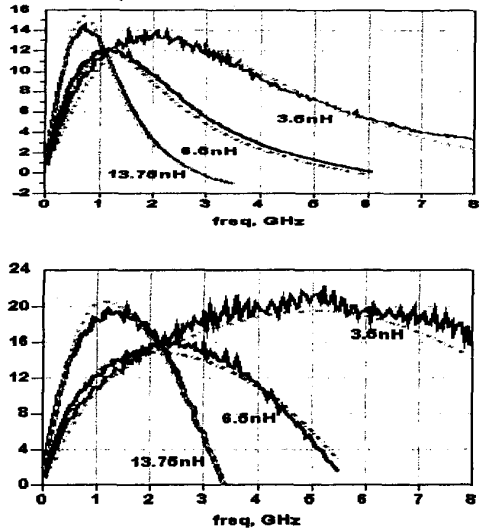

Fig. 8. Measured (solid line) vs. modeled (doted line) one-port single-ended (top) and differential (bottom) Q of three-port inductors

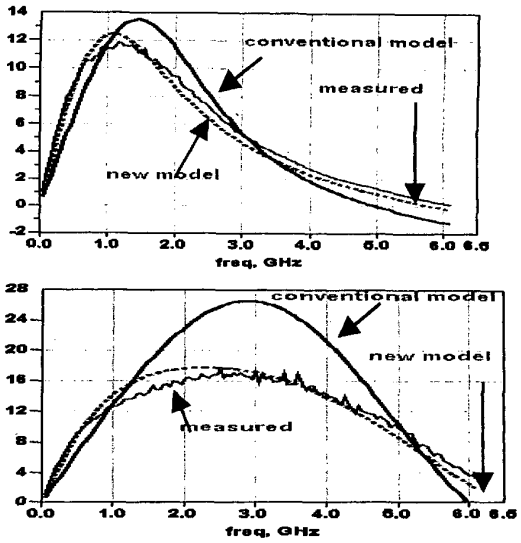

Fig. 9. 1-port single ended (top) and differential (bottom) Q of a 6.5nH 3-port inductor.

IV. CONCLUSION

New inductor model forms for two-port and three-port silicon integrated inductors have been developed. These models utilize frequency independent lumped elements to mimic the skin effect behavior of transmission lines on silicon. In addition they can also be integrated in harmonic balanced and time domain simulators, and therefore enabling the modeling of non-linear effects in linear environments.

ACKNOWLEDGMENT

The authors would like to thank Tammie Teraji, Rampi Ramprasad, Rashaunda Henderson, Yingying Yang and other members of the AMMS team for the various technical discussions.

REFERENCES

[1] C.P. Yue, S.S. Wong, "Physical Modeling of Spiral Inductors on Silicon", *IEEE Transactions on Electron Devices, Vol. 47*, No. 3, March 2000, pp. 560-568

[2] S. Kim, D.P. Neikirk, "Compact Equivalent Model for the Skin effect", *Microwave Symposium Digest, 1996, IEEE MTT_S International, Volume 3*, pp. 1815-1818

[3] S. Ramo, J.R. Whinnery, T. Van Duzer, *Fields and Wave in Communication Electronic"*, New-York:Wiley, 3rd Edition, pp 149-153

[4] L.J. Giacoletto, "Frequency- and Time-domain analysis of skin effect", *IEEE transactions on magnetics, vol. 22, No 1*, January 1996, pp. 220-229